Am J Cancer Res 2022;12(11):4988-5003
www.ajcr.us /ISSN:2156-6976/ajcr0144203

Original Article

TRIM27 is an adverse prognostic biomarker and associated with immune and molecular profiles in right-sided colon cancer

Minghui Zhang[1,2,3,4], Bowen Yang[1,2,3,4], Lingyun Zhang[1,2,3,4], Xiaoyu Guo[1,2,3,4], Guangwei Zhang[5], Xiaofang Che[1,2,3,4], Ce Li[1,2,3,4], Kezuo Hou[1,2,3,4], Xiaojie Zhang[1,2,3,4], Jinglei Qu[1,2,3,4], Ti Wen[1,2,3,4], Xiujuan Qu[1,2,3,4]

[1]Department of Medical Oncology, The First Hospital of China Medical University, Shenyang 110001, Liaoning, China; [2]Key Laboratory of Anticancer Drugs and Biotherapy of Liaoning Province, The First Hospital of China Medical University, China Liaoning Province Clinical Research Center for Cancer, Shenyang 110001, Liaoning, China; [3]Liaoning Province Clinical Research Center for Cancer, Shenyang 110001, Liaoning, China; [4]Key Laboratory of Precision Diagnosis and Treatment of Gastrointestinal Tumors, Ministry of Education, Shenyang 110001, Liaoning, China; [5]Smart Hospital Management Department, The First Hospital of China Medical University, Shenyang 110001, Liaoning, China

Received May 16, 2022; Accepted October 26, 2022; Epub November 15, 2022; Published November 30, 2022

Abstract: Right-sided colon cancer (RCC), as an independent tumor entity, shows a poor prognosis. It is imperative to detect immune microenvironment-related genes for predicting RCC patient prognosis and study their function in RCC. Tripartite motif-containing 27 (TRIM27) was identified as a risk signature from The Cancer Genome Atlas (TCGA) and the Gene Expression Omnibus (GEO) datasets by using weighted gene co-expression network analysis, differentially expressed analysis, and univariate Cox analysis. It predicted a poorer overall survival and increased lymph node metastasis, which were then validated in our 48 clinical samples. Using immunohistochemistry, TRIM27 was found to be highly expressed in both cancer cells and surrounding immunocytes, and its expression in tumor or immune cells both predicted a poorer prognosis. Thereafter, the functional mechanism, immune and molecular characteristics of TRIM27 were investigated using gene set enrichment analysis (GSEA), ESTIMATE, CIBERSORT, and gene set variation analysis (GSVA) at the single-cell, somatic mutation, and RNA-seq level. Patients with highly expressed TRIM27 presented lower $CD4^+$ T cell infiltration and activation of the mTORC1/glycolysis pathway. In addition, patients with highly expressed TRIM27 were characterized by hypermetabolism, higher tumor purity, more BRAF mutation, and more chromosomal instability. Collectively, TRIM27 is an important immune-related prognostic biomarker in patients with RCC. It may function via activating the mTORC1/glycolysis pathway and suppressing $CD4^+$ T cells. These results indicated that TRIM27 could be a promising therapeutic target in RCC.

Keywords: Right-sided colon cancer, tripartite motif-containing 27, immune related gene, prognostic biomarker, $CD4^+$ T infiltration

Introduction

Colorectal cancer (CRC) is the second major cause of cancer mortality globally [1]. Growing evidence indicates that significant varieties, including carcinogenesis mechanisms, clinical characteristics, and response to treatment exist between right-sided (RCC) and left-sided colon cancer (LCC) [2, 3]. Most research finds that RCC patients have a poorer prognosis and inferior benefits accrue from cetuximab treatment than in LCC patients [4, 5], which may lead to more aggressive therapies, including triplet chemotherapy and bevacizumab [3, 6]. Consequently, we aimed to investigate valuable prognosis biomarkers in RCC, as an independent tumor.

With the development of precision medicine, some researchers have focused more on RCC and found that lymph node status and circulating $CD4^+$ T cells could affect RCC prognosis [7, 8]. As an indispensable component of tumor biology, the tumor immune microenvironment (TIME) has received increasing attention because it is a crucial prognostic indicator and

acts in enhancing responsiveness to treatment schemes including immunotherapy [9-11]. Compared to LCC, TIME in RCC is characterized by increased immunogenicity, higher immune activity, and higher intraepithelial T cell infiltration, which implies a significant role of TIME-related genes in RCC prognosis [12]. Several immune-related genes that are associated with overall prognosis of CRC have been identified [13]. However, the mechanism of influence of TIME on the prognosis of RCC remains elusive. Hence, it is suitable to evaluate the influence of TIME-related genes on prognosis and determine biomarkers for precisely predicting prognosis and guiding personalized therapy in RCC patients.

Tripartite motif-containing 27 (TRIM27), which inherits the basic structure of the TRIM family, is composed of a RING finger domain, one or two B-box domains, and a coiled-coil domain [14]. It possesses E3 ubiquitin ligase capability and is involved in transcriptional repression, negative regulation of apoptosis, improving cell viability, proliferation, migration, and invasion [15]. TRIM27 is highly expressed in specific tumors, including hepatocellular carcinoma, esophageal cancer, gastric cancer, and so on [16-20]. In CRC, TRIM27 promotes colitis-associated carcinogenesis and epithelial-mesenchymal transition (EMT) [21, 22]. Besides, it has been reported to enhance chemotherapy resistance to cisplatin [23]. However, the exact role of TRIM27 in RCC patients remains to be fully determined.

In this study, TRIM27 was found to be an immune-related prognostic biomarker in RCC patients. Its high expression foreshadowed a poor prognosis, a hypermetabolic state, and a lower infiltration level of $CD4^+$ T cells. TRIM27 possibly suppresses the infiltration of $CD4^+$ T cells in RCC and has potential value in predicting prognosis and improving treatment outcomes, especially immunotherapy.

Materials and methods

Data acquisition

CRC samples located in the cecum, ascending colon and hepatic flexure of the colon were included in our study. The RNA-seq count data and clinical information of 195 RCC samples were obtained from The Cancer Genome Atlas (TCGA, https://portal.gdc.cancer.gov/projects). The raw counts were first normalized to transcripts per million (TPM) and then transformed to log2(x+1). RNA-seq data of 224 RCC samples (GSE39582) were downloaded from the Gene Expression Omnibus datasets (GEO, https://www.ncbi.nlm.nih.gov/geo/). The immune-related genes were obtained from the ImmPort database (https://immport.niaid.nih.gov) [24]. The molecular subtypes of 145 RCC samples were downloaded from a molecular analysis of gastrointestinal adenocarcinomas [25].

Identification of hub immune-related genes

Gene modules highly correlated with RCC patients were analyzed using the "WGCNA" R package among the genes with a maximum 80% variance. A weighted co-expression relationship was initially built based on the adjacency matrix by using pairwise Pearson correlation analysis. The topological overlap matrix (TOM) describing the similarity between genes was then transformed. 1-TOM was used as the distance to cluster the genes, and the modules were merged at a threshold of 0.25. Then, genes in the modules which significantly associated with RCC were selected for further differential expression analysis.

Differently expressed genes (DEGs) between RCC and normal samples were identified using the "edgeR" R package in the TCGA cohort. |log2 fold change| > 1 and false-discovery rate (FDR) < 0.05 were considered as the cut-off thresholds. Also, DEGs in GSE39582 datasets were obtained using the "limma" R package with the threshold of fold change > 1.5 and adjusted *P*-value < 0.05. After taking the intersection of the DEGs from TCGA-RCC and GSE39582 cohorts, 22 hub genes were obtained and analyzed using Gene Ontology (GO) with the "clusterProfiler" package of R.

Validation of TRIM27's prognostic value

Using the "survival" R package, a univariate Cox regression analysis was applied to identify that TRIM27 was a gene significantly affecting RCC prognosis. Then, the patients in the TCGA cohort were divided into two groups according to the best cut-off through receiver operating characteristic (ROC) analysis. Subsequently, we used Kaplan-Meier survival analysis to assess the prognostic value of the TRIM27 in both

TCGA and our cohorts. DEGs were obtained between patients with high and low expression levels of TRIM27 and then KEGG pathways were identified using "ggplot2", "clusterProfiler", and "GSEABase" R packages.

Immune infiltration characteristics of patients with high and low levels of TRIM27

To identify TIME characteristics in the patients with high and low levels of TRIM27, we performed three standard methods to elevate immune infiltration levels: (1) The "ESTIMATE" package was used to calculate the stromal score, immune score, and tumor purity [26]. (2) CIBERSORT (https://cibersort.stanford.edu/) was performed to estimate the relative proportion of 22 types of immune cells [27]. (3) The "GSVA" R package was used to perform gene set variation analysis (GSVA) and reveal the distinction of 28 types of lymphocyte characterization between different TRIM27 subgroups [28]. The certain immune-related signatures of 28 lymphocytes were obtained from Charoentong's study [29].

Molecular characteristics in the groups with high and low levels of TRIM27

We obtained genes mutated most frequently in colon cancer according to previous studies [30]. Subsequently, the quantity and quality of gene mutations were performed using the "GenVisR" R package. The "maftools" R package was then used to calculate the total number of somatic non-synonymous point mutations within each sample. Then, the correlation between TRIM27 and immune check inhibitors (ICIs) was analyzed. Referring to existing studies, we chose five ICIs, including programmed death-ligand 1 (PD-L1), programmed death 1 (PD-1, also known as PDCD1), T cell immunoglobulin domain and mucin domain-containing molecule-3 (TIM-3, also known as HAVCR2), indoleamine 2,3-dioxygenase 1 (IDO1), and cytotoxic T-lymphocyte-associated protein 4 (CTLA-4).

Distribution and GSEA of TRIM27 at the single-cell level

The single-cell RNA-sequencing (scRNA-seq) data were downloaded from the GEO database (GSE132465) [31]. scRNA-seq in 11 RCC samples were clustered as a standard process using "Seurat" package. The cells with less than 200 UMIs or with more than 10% mitochondrion-derived UMI counts were considered low-quality cells and removed. With parameter "principal components" = 20, "resolution" = 0.5, the "FindClusters" function was used to identify cell clusters and annotate each subpopulation by known biomarkers in straightforward analysis and the CellMarker database (http://xteam.xbio.top/CellMarker/) [32, 33]. Markers used in this study are listed: cancer cells (EPCAM, KRT8), T cells (CD3E, CD3E), $CD4^+$ T cells (ICOS, TRAT1), $CD8^+$ T cells (CD8A, CD8B), regulatory T (Treg) cells (FOXP3), B cells (CD79A, CD19), endothelial cells (VWF, ENG), fibroblasts (COL1A1, COL3A1, DCN), myeloid cells (CD68), plasma cells (MZB1, IGLC3), dendritic cells (LILRA4, CLEC4C), mast cells (TPSB2), basal cells (KRT6A, KRT17). Then, cell clusters were visualized using uniform manifold approximation and projection (UMAP) map, which was the most popular algorithm for the reduction of data dimensions. According to the expression of TRIM27 on tumor cells, we considered patient 1, patient 3, patient 6, patient 9, and patient 11 as the highly expressed TRIM27 group and the other patients as the lowly expressed TRIM27 group. Furthermore, we extracted specific subpopulations and performed gene set enrichment analysis (GSEA) based on the HALLMARK gene sets ($P < 0.05$ and FDR < 0.25) to explore the function of TRIM27.

Tissue samples and immunohistochemistry

This study was reviewed and approved by the Ethics Committee of the First Affiliated Hospital of China Medical University (ethics batch number: 2019-157). 48 RCC patients who underwent surgery between October 2010 and August 2012, in the First Hospital of China Medical University, were included in our study. All patients were aged between 36 to 81 years, with a median of 67 years. In total, 48 RCC sections and 20 paired adjacent normal sections were collected.

To detect the expression level of TRIM27 in RCC, TRIM27 staining was carried out using the UltrasensitiveTM SP immunohistochemistry kit (Maxim (China) KIT-9720). These sections were deparaffinized and rehydrated in xylene and gradients of ethanol (100%, 95%, and 75%) followed by heat-mediated antigen retrieval in

citrate buffer. The sections were washed in phosphate-buffered saline (PBS) three times and were placed in 0.3% hydrogen peroxide (H_2O_2) for 20 min, followed by three washes with PBS. The tissues were then soaked in the non-specific staining blocker for 30 min. Finally, the tissues were reacted with anti-TRIM27 antibodies (diluted 1:500, polyclonal, rabbit, ab78393; Abcam, Cambridge, USA) overnight at 4°C, followed by incubation with biotin-labeled secondary antibody and streptavidin-linked peroxidase at room temperature for 5 min, and with the color agent diaminobenzidine. The nuclei were counterstained with hematoxylin, and the sections were dehydrated using different grades of ethyl alcohol and xylene. Based on the staining intensity, the level of TRIM27 was graded as 0 (no staining), 1 (+), 2 (++), and 3 (+++). According to the proportion of TRIM27-positive cells, the positive rate was scored as 0 (negative), 1 (< 30%), 2 (31-60%), and 3 (> 60%). The total score was calculated as the intensity score plus the positive rate score. Score > 4 in cancer cells or score > 8 in immune cells were both regarded as highly expressed TRIM27 samples.

Statistics

The correlation between data with a normal distribution was analyzed with Pearson's correlation analysis. One-way ANOVA or Student's t-test was used to determine the significance of differences between the gene expression and clinicopathological characteristics. The Wilcox test was used to compare the immune cell infiltration levels between different TRIM27 subgroups. Categorical data were tested using the Chi-square test, but Fisher's exact test was adopted when sample sizes were small. All the statistical analysis results described below were obtained with the R software. The significance level was set to $P < 0.05$.

Results

Identification of RCC immune-related hub genes from TCGA and GSE39582 cohorts

The workflow pertaining to the present study was shown in **Figure 1**. To obtain RCC immune-related hub genes, this research first analyzed 1131 immune-related genes through the weighted gene co-expression network analysis (WGCNA) in two cohorts: TCGA and GSE39582. The optimal soft-thresholding powers based on the scale-free network were five and three respectively (Figure S1). In the TCGA cohort, two RCC-related modules (a red module (r = 0.95, $P < 0.001$) and a green module (r = 0.81, $P < 0.001$)) were determined, and 180 genes could be eventually obtained (**Figure 2A-C**). Among these, 151 RCC hub genes were differentially expressed in RCC and normal colon samples (46 up-regulated genes and 105 down-regulated genes) (**Figure 2D**). Meanwhile, 110 RCC hub genes in the yellow module (r = 0.84, $P < 0.001$) were screened out in another GSE39582 cohort (**Figure 2E**, **2F**) and 68 genes were differentially expressed in RCC and normal colon samples (22 up-regulated genes and 46 down-regulated genes) (**Figure 2G**).

Finally, 22 candidate genes were acquired by taking the intersection of hub genes in TCGA-RCC and GSE39582 (**Figure 3A**). GO analysis showed these 22 genes were correlated with the biological processes (BP) including negative regulation of interleukin-2 production, negative regulation of tumor necrosis factor (TNF) production, extracellular-signal-regulated kinase 1 (ERK1) and extracellular-signal-regulated kinase 2 (ERK2) cascade, T cell differentiation, and so on (Figure S2A). A heatmap and a table describing these 22 gene expression levels in RCC are provided (Figure S2B, S2C and Table S1).

TRIM27 predicted a poorer prognosis in RCC patients

To verify the key prognosis-related genes among the 22 genes, a univariate Cox regression analysis was performed on the TCGA cohort. The result indicated that TRIM27 was a significant risk factor (HR = 2.527, 95% CI (1.235-5.170), P = 0.011) (**Figure 3B**). Analytical results were provided in Table S2. TRIM27 was more highly expressed in RCC samples compared to normal colon samples (**Figure 3C**). TCGA patients were then stratified into the highly and lowly expressed groups of TRIM27 according to the best cut-off of 5.087 (**Figure 3D**). This finding revealed that TRIM27 was significantly correlated with higher mortality ($P = 1.077 \times 10^{-3}$) in a Kaplan-Meier survival analysis (**Figure 3E**, **3F**).

Subsequently, TRIM27 was detected using our samples including 48 colorectal cancer tissues

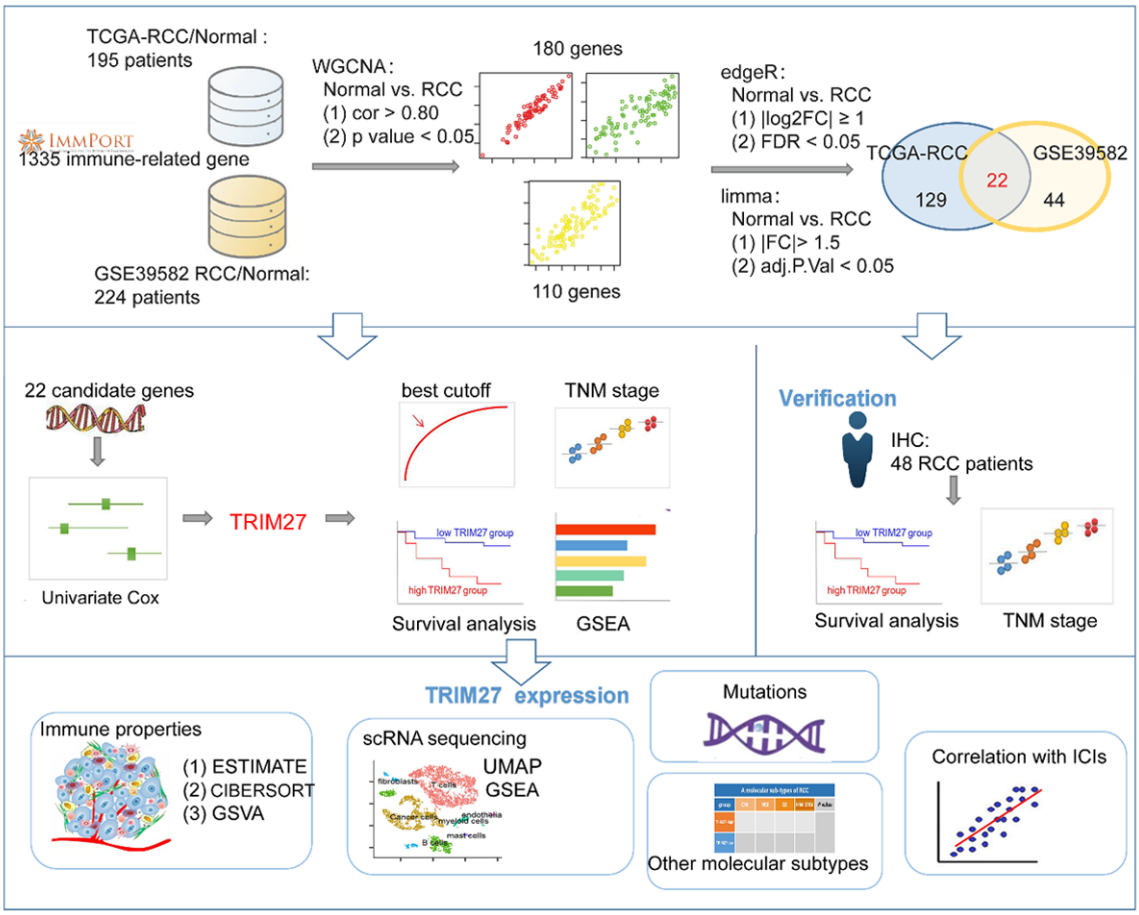

Figure 1. Graphical abstract for the identification of TRIM27 correlated with poor survival in RCC.

and 20 normal colon tissue specimens and the result verified that at the protein-level, TRIM27 was up-regulated in RCC. Interestingly, TRIM27 was not merely expressed in cancer cells but also in surrounding immune cells (**Figure 3G**) and the Kaplan-Meier survival analysis also proved that TRIM27 predicted a poorer prognosis (P = 0.009) (**Figure 3H**). The same results could be observed separately in cancer cells or immune cells (Figure S3).

To investigate the relationship between TRIM27 and TNM clinicopathological classification, the TCGA cohort and our 48 RCC patients were further analyzed. In the TCGA cohort, higher expression of TRIM27 was associated with increased lymph node metastasis, but no significant association with invasion, distal metastasis, or tumor stage was found (**Figure 4A-D**). Consistent with the TCGA cohort, the same results were found from our 48 RCC patients (**Table 1**). To reveal the potential functional mechanism of TRIM27 in RCC, a GSEA was conducted. Metabolism-related KEGG pathways, especially the pentose phosphate pathway, could be activated and "mismatch repair" was depressed in patients with high TRIM27 expression; while many metabolism-related pathways were depressed in patients with low TRIM27 expression (**Figure 4E**, **4F**). These findings indicated the patients with high TRIM27 expression were characterized by a hypermetabolic state, which met the energy needs for tumor proliferation.

Immune infiltration characteristics of patients with high and low levels of TRIM27

To reveal the difference of immune infiltration in the patients with high and low levels of TRIM27, the proportions of stromal and immune cells of patients in TCGA cohort were evaluated and we found that the patients with low TRIM27 expression presented higher stromal cell and

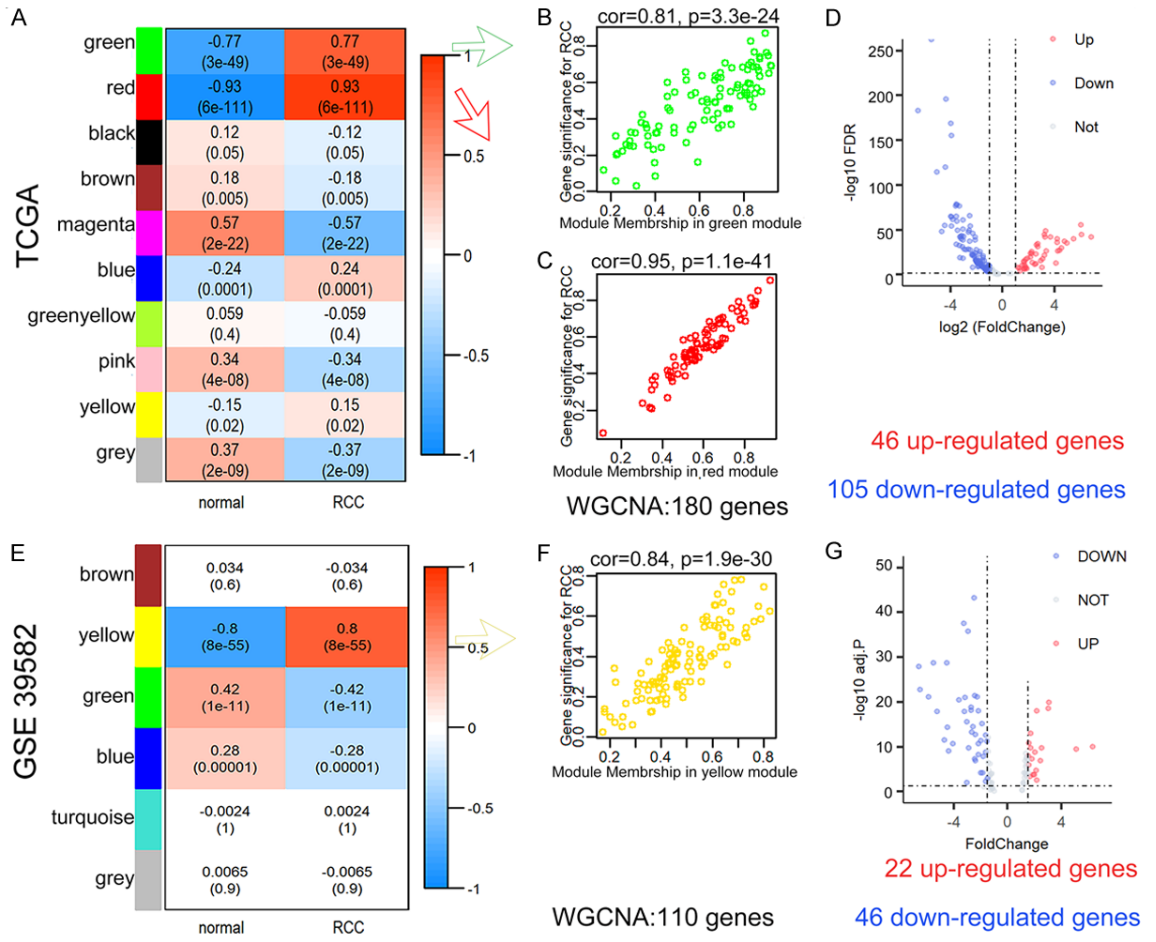

Figure 2. Identification of RCC immune-related hub genes. A. Gene modules obtained by WGCNA in TCGA cohort (normal *vs.* RCC). B, C. Scatter plot of green (r = 0.81, P < 0.001) and red modules (r = 0.95, P < 0.001). D. Volcano map of DEGs in green and red modules (up-regulated genes in red and down-regulated genes in blue). E. Gene modules obtained by WGCNA in the GSE39582 cohort (normal *vs.* RCC). F. Scatter plot of yellow module (r = 0.84, P < 0.001). G. Volcano map of DEGs in the yellow module.

immune cell infiltration while the patients with high TRIM27 expression demonstrated higher tumor purity (**Figure 5A-C**). Then, the relationship between TRIM27 and the immune component was determined. Plasma cells, resting memory CD4$^+$ T cells, and resting dendritic cells were found to be fewer in number while M0 and M1 macrophages were more abundant in the patients with high TRIM27 expression (**Figure 5D**).

To study the correlation between TRIM27 and kinds of immune cells, GSVA was used to calculate the proportions of 28 lymphocytes within each sample. The result was visualized in a heat map (**Figure 5E**). Pearson's correlation results implied that the level of TRIM27 expression was negatively associated with activated B cells (r = -0.22; P = 0.0021), Type-1 T-helper cells (r = -0.16; P = 0.034), mast cells (r = -0.22; P = 0.0022), and neutrophils (r = -0.18; P = 0.016). Detailed results of Pearson analysis were displayed in Table S3. Thus, it was speculated that immune cells, especially CD4$^+$ T cells, exhibited a lower level of infiltration in the patients with high TRIM27 expression.

Distribution of TRIM27 and its action on CD4$^+$ T cells in RCC scRNA-seq

The workflow of TRIM27 in scRNA-seq was displayed (**Figure 6A**). To explore the heterogeneity of TRIM27 at the single-cell level, 11 RCC patients were included and 12 cell types were identified in the present study (**Figure 6B**, **6C**). TRIM27 was shown to exhibit heterogeneity

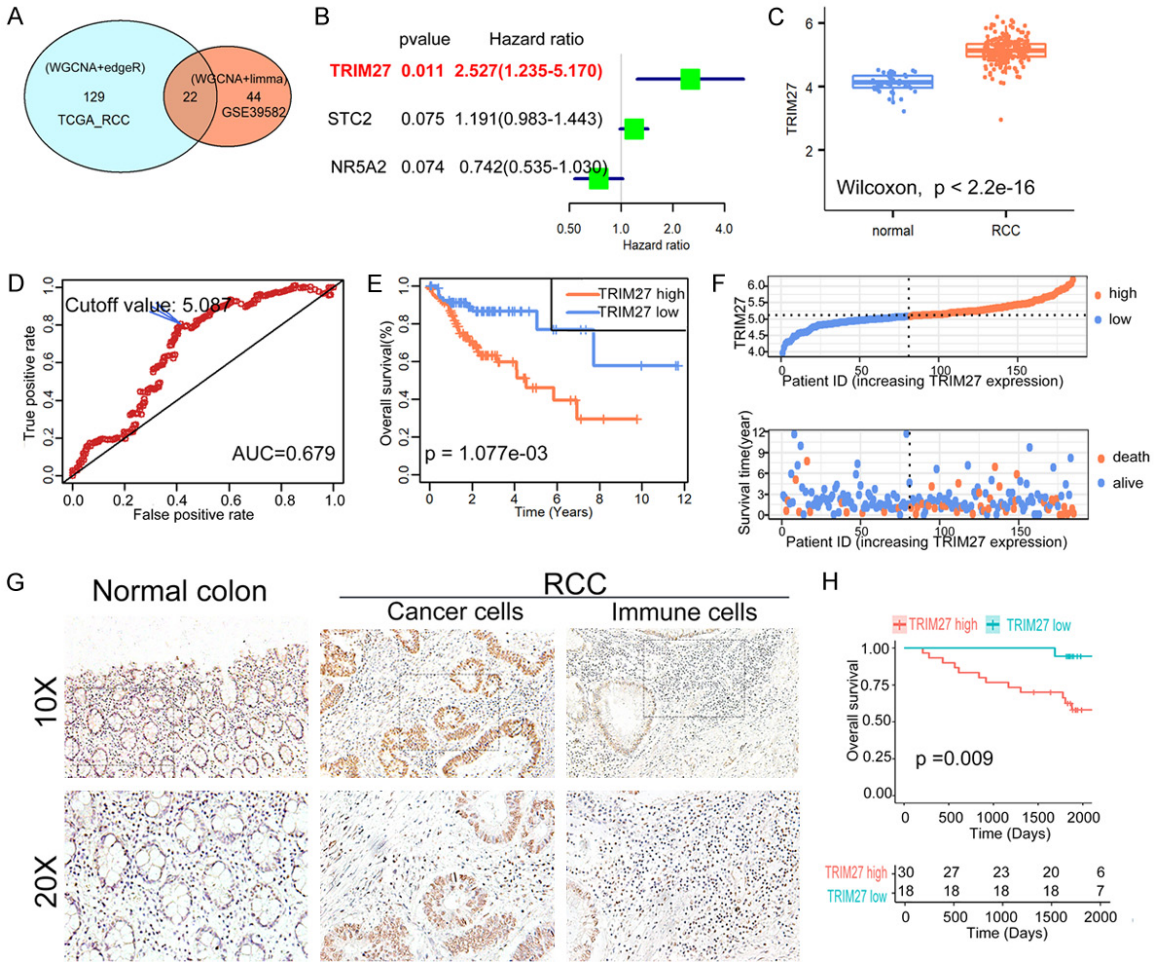

Figure 3. Identification and survival analysis of TRIM27. A. The intersection of immune-related hub genes in TCGA-RCC and GSE39582. B. Univariate Cox analysis of 22 immune-related hub genes. C. The expression of TRIM27 in RCC and adjacent normal samples in TCGA. D. ROC analyses based on the expression level of TRIM27. E. Kaplan-Meier survival analysis of the highly and lowly expressed groups of TRIM27. F. Distribution of TRIM27 expression levels and survival status of RCC patients in the TCGA cohort. G. Verification of TRIM27 expression in normal colon and RCC tissues by immunohistochemical assay. H. Kaplan-Meier survival analysis of TRIM27 in 48 RCC patients.

among different patients and cell types (**Figure 6D**, **6E**). The expression levels of TRIM27 on tumor cells in the group with high TRIM27 expression (patient 1, patient 3, patient 6, patient 9, and patient 11) and the group with low TRIM27 expression (patient 2, patient 4, patient 5, patient 7, patient 8, and patient 10) were significantly different ($P < 0.001$) (**Figure 6F**). Tumor purity and immune cell infiltration were observed differently in the highly and lowly expressed groups of TRIM27, from which the proportion of $CD4^+$ T cells was most significantly different. Compared to the group with low TRIM27 expression, $CD4^+$ T cells in the group with high TRIM27 expression were significantly lower (8.6% *vs.* 26.5%, $P = 0.013$) (**Figures 6G**, **6H**, S4). This reflected the same result as the TCGA analysis.

The results indicated that the TRIM27 in cancer cells influenced prognosis of RCC patients and negatively regulated $CD4^+$ T cell infiltration, the potential function of TRIM27 in cancer cells was assessed. GSEA analysis implied that "MTORC1 signaling", "MYC targets", and "glycolysis" were enriched in the cells with high TRIM27 expression (**Figure 6I**). These results suggested high expression of TRIM27 in cancer cells might play a function via these pathways to suppress the infiltration of $CD4^+$ T cells, thus affecting the prognosis. All enriched pathways were listed in Table S4. In addition, we also

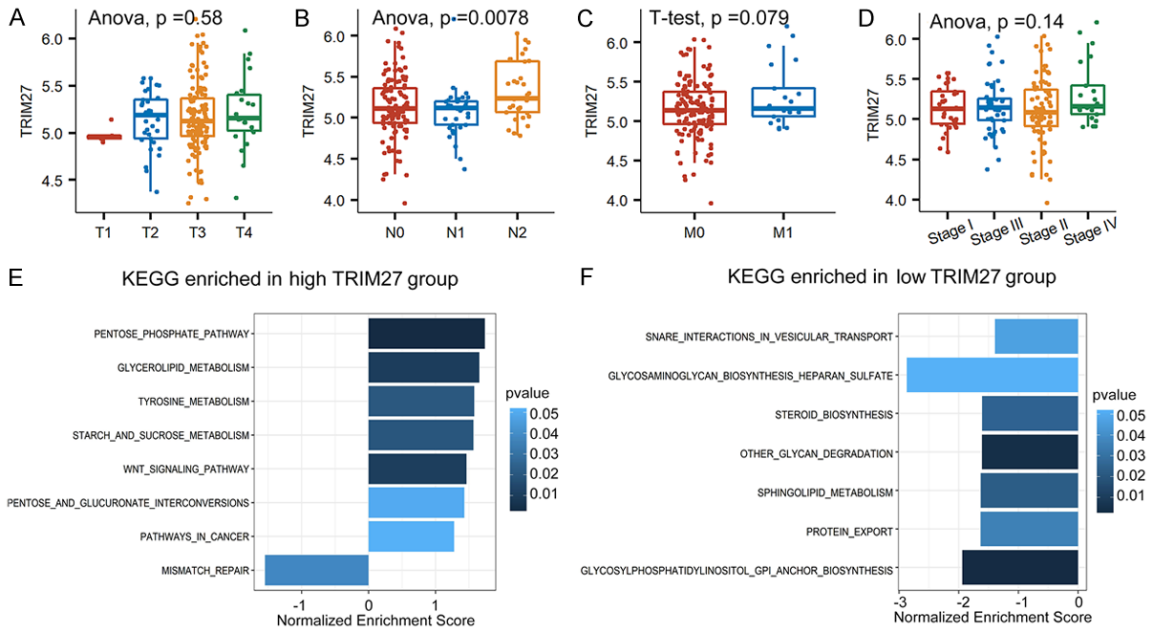

Figure 4. The relationship of clinical characteristics and KEGG pathway with TRIM27. (A) Expression of TRIM27 based on T (A), N (B), M (C), and clinicopathological stages (D). KEGG pathways enriched in the highly and lowly expressed groups of TRIM27 (E, F).

Table 1. The relationship between the level of expression level of TRIM27 and the clinicopathological characteristics of RCC patients

	High TRIM27 (N = 30)	Low TRIM27 (N = 18)	*P* Value
Sex			0.762
F	12 (40.0)	6 (33.3)	
M	18 (60.0)	12 (66.7)	
Age			0.375
≤65	12 (40.0)	10 (55.6)	
> 65	18 (60.0)	8 (44.4)	
Stage			0.329
Stage II	14 (53.8)	10 (71.4)	
Stage III	12 (46.2)	4 (28.6)	
T			0.506
T1	0 (0.0)	1 (5.9)	
T2	5 (16.7)	3 (17.6)	
T3	25 (83.3)	13 (76.5)	
M			1
M1	24 (96.0)	11 (91.7)	
M2	1 (4.0)	1 (8.3)	
N			0.049*
N1	13 (43.3)	14 (77.8)	
N2	12 (40.0)	4 (22.2)	
N3	5 (16.7)	0 (0.0)	

*: $P < 0.05$.

found TRIM27 expressed in both tumor cells and surrounding immune cells including $CD4^+$ T cells, $CD8^+$ T cells, myeloid cells, plasma cells, and so on. Among these cells, the TRIM27 level was higher in tumor cells, plasma cells, myeloid cells, endothelial cells, fibroblasts, $CD4^+$ T cells, and $CD8^+$ T cells, whereas was lower in Treg, mast, and basal cells (**Figure 6E**).

Molecular characteristics of the groups with high and low levels of TRIM27

Aiming at further biological insight into TRIM27, a gene mutation analysis was performed to explore the relationship between TRIM27 and other molecular subtypes. In general, in RCC patients, missense mutation variation was the most common mutation type and among the mutation genes reported in the previous studies. The adenomatous polyposis coli (APC) gene, as a tumor suppressor gene, was the most common mutation gene (**Figure 7A**, **7B**). We also found that in the patients with high TRIM27 expression, BRAF mutation was higher ($P = 0.031$) (**Figure 7C**), however, APC mutation and tumor mutation burdens were not significantly different in the highly and lowly expressed groups of TRIM27 (Figure S5A, S5B).

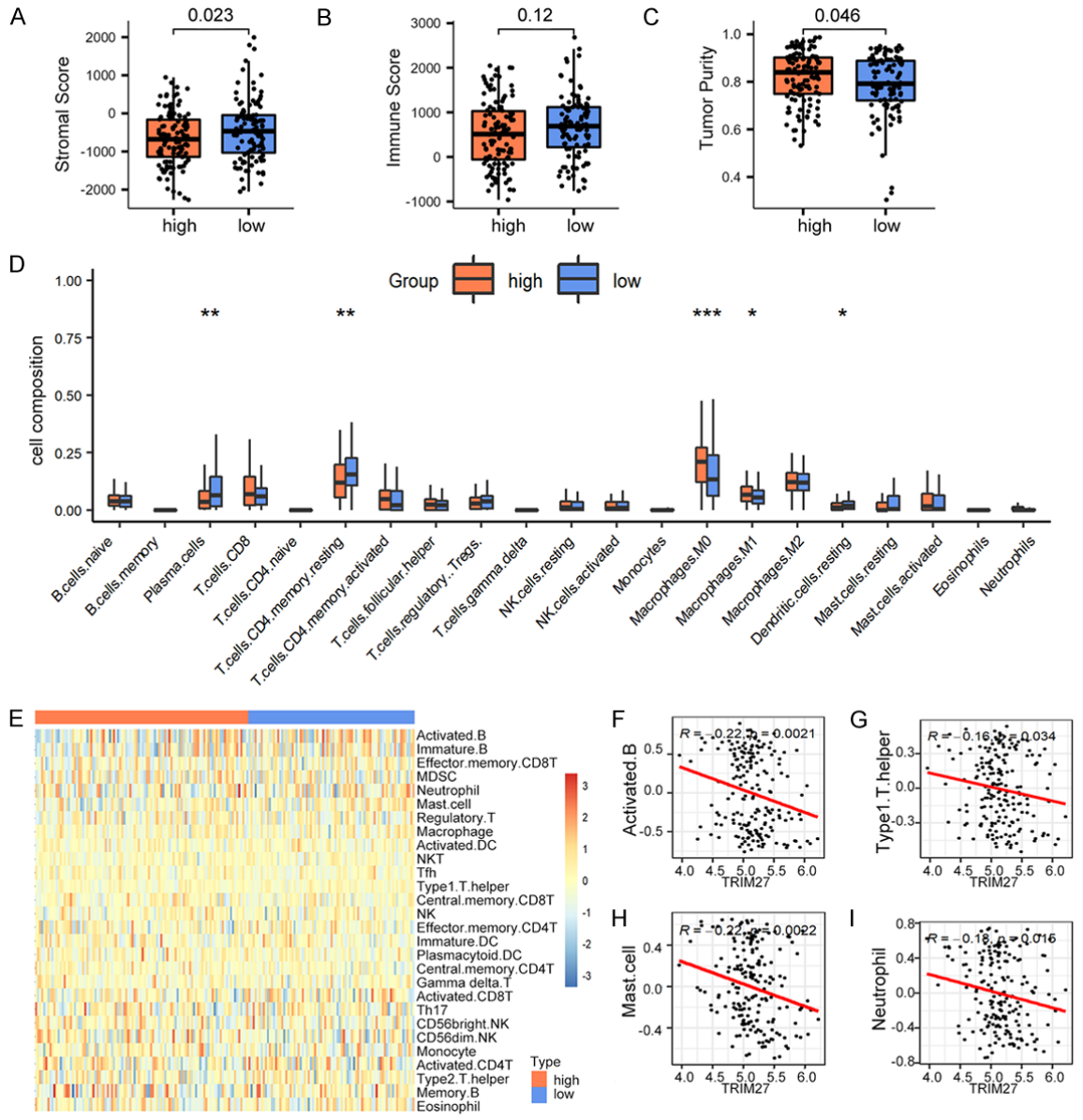

Figure 5. Immune infiltration characteristics of the patients with high and low levels of TRIM27. Stromal score (A), immune score (B) and tumor purity (C) in the patients with high and low levels of TRIM27. (D) Comparison of immune cell composition in the patients with high and low levels of TRIM27 (*P < 0.05, ** P < 0.01, *** P < 0.001). (E) A heatmap of 28 TILs for TCGA patients. The groups with high and low levels of TRIM27 were shown as patient annotations. (F-I) The correlation between TRIM27 expression level and TILs.

Then 145 RCC samples were further classified based on four molecular features subtypes: hypermutated-single-nucleotide variant predominant (HM-SNV), microsatellite instability (MSI), chromosomal instability (CIN), and genomically stable (GS). As shown in **Figure 7D**, the highly expressed group of TRIM27 comprised 50 CIN samples, 23 MSI samples, six GS samples, and two HM-SNV samples, while the low-TRIM27 group included 33 CIN samples, 15 MSI samples, and 16 GS samples. CIN samples and fewer GS samples in the highly expressed group of TRIM27 (P = 0.015) could be found. CIN is a hallmark associated with poor prognosis, metastasis, and therapeutic resistance and these results are consistent with the Kaplan-Meier survival analysis. Significant differences of other molecular subtypes reported before such as the consensus molecular subtype (CMS) classification, CpG

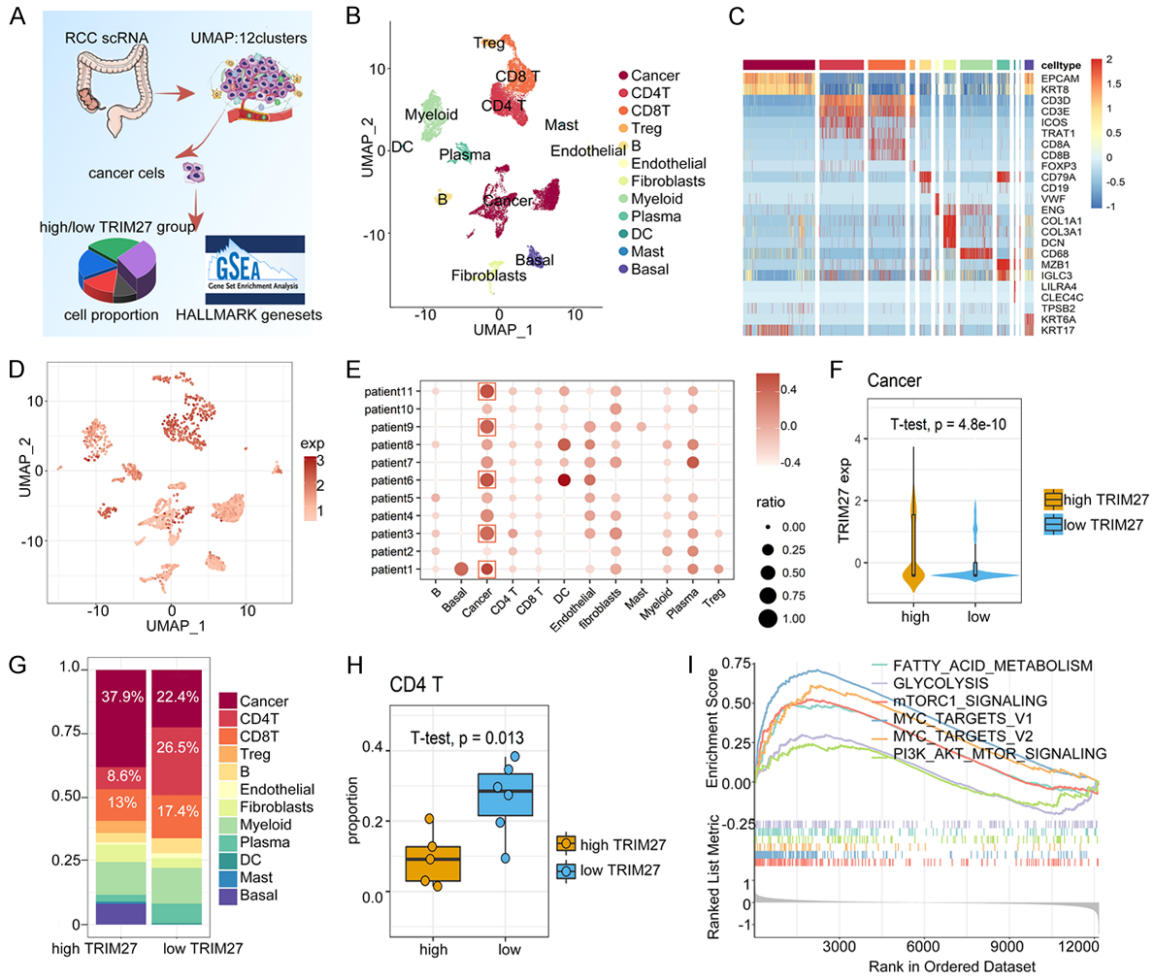

Figure 6. Distribution of TRIM27 and its action on CD4⁺ T cells in scRNA-Seq data. (A) An analysis workflow for TRIM27. (B, C) UMAP plot of 21,289 cells in the GSE132465 dataset and 12 cell clusters identified by canonical marker gene expression. (D, E) Distribution of TRIM27 in identified cell types and patients. (F) The expression level of TRIM27 on cancer cells in high-TRIM27 (patient 1, patient 3, patient 6, patient 9, and patient 11) and low-TRIM27 group (patient 2, patient 4, patient 5, patient 7, patient 8, and patient 10). (G) The proportions of various cell types in the highly and lowly expressed groups of TRIM27, among which CD4⁺ T cells were most significantly different (P = 0.013) (H). (I) GSEA of TRIM27 in cancer cells.

island methylator phenotype (CIMP)-H/CIMP-L/Non-CIMP, and MSI-H/MSI-L/Microsatellite stability (MSS) classification, were not observed in the highly and lowly expressed groups of TRIM27 (Figure S5C-E).

Since the levels of expression of immune checkpoint genes might be related to the clinical outcome of immunotherapy, the correlations between the TRIM27 and immune checkpoint genes were evaluated using Pearson correlation. The results showed that TRIM27 had a significantly positive correlation with CTLA4 (r = 0.22; P < 0.001) and a slightly positive correlation with PDCD1 (r = 0.17; P = 0.011), IDO1 (r = 0.13; P = 0.046), and HAVCR2 (r = 0.13; P = 0.057) (**Figure 7E-H**). These findings suggested tumor immune escape might be involved in TRIM27-mediated carcinogenesis of RCC and the patients with high TRIM27 expression could benefit from immunotherapy.

Discussion

Previous reports have shown TRIM27 ubiquitinated and degraded various substrates such as PTEN, p21, and SIX3 [18, 19, 34, 35]. As an E3 ubiquitin ligase, it is related to the development of specific tumors, including esophageal cancer, gastric cancer, lung cancer, and so on.

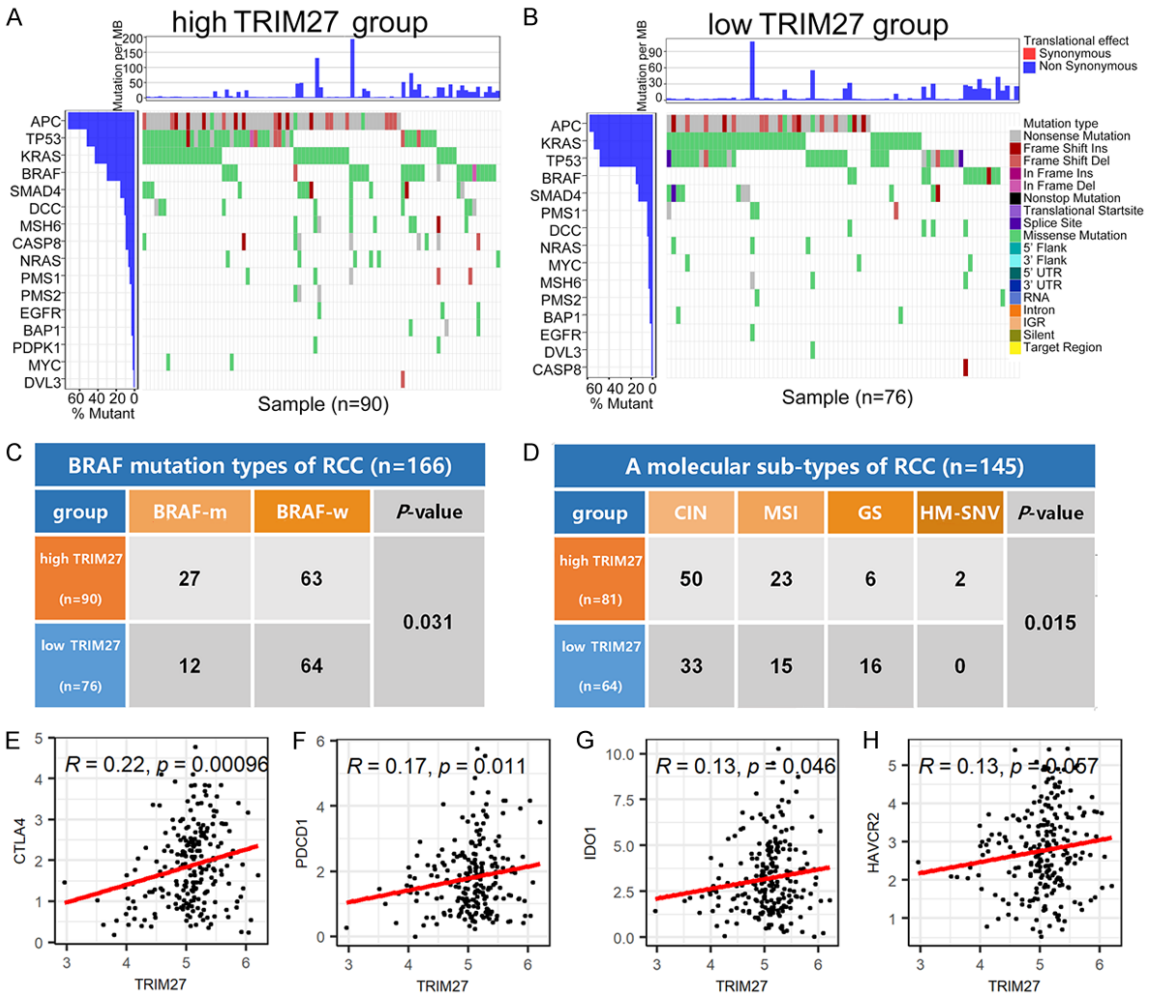

Figure 7. Molecular characteristics of the highly and lowly expressed groups of TRIM27. (A, B) Significantly mutated genes in the mutated RCC samples the highly and lowly expressed groups of TRIM27. Mutated genes (rows) are ordered by the mutation rate; samples (columns) are arranged to emphasize mutual exclusivity among mutations. The color coding indicates the mutation type. (C) Table showing the distribution of BRAF mutation subtypes between the highly and lowly expressed groups of TRIM27. (D) Table showing the distribution of molecular subtypes (CIN, MSI, GS, and HM-SNV) between the highly and lowly expressed groups of TRIM27. Correlation between TRIM27 and expression level of ICIs: CTLA4 (E), PDCD1 (F), IDO1 (G), and HAVCR2 (H).

A recent study reported that TRIM27 could promote EMT and activate phosphorylated AKT serine/threonine kinase in human colon cancer cell lines [22]. The results were consistent with the findings of the present study such that higher TRIM27 expression foreshadowed poor prognosis and lymph node metastasis in colon cancer. Importantly, RCC has a poorer prognosis, and significant differences in carcinogenic mechanisms, clinical characteristics, and treatment schemes compared to LCC. Thus, RCC was considered as an independent tumor entity to explore the expression, distribution, and biological process of TRIM27 in RCC.

We found TRIM27 was not only expressed in tumor cells but also in surrounding immune cells. Furthermore, its level of expression in immunocytes was also related to RCC prognosis, indicating that TRIM27 might regulate tumor immunity through an unknown mechanism. To explore its potential mechanism, we conducted ESTIMATE analysis and found that the infiltration of immune cells was negatively correlated with TRIM27, suggesting the mechanism of TRIM27 resulted in a poorer prognosis. To test this hypothesis, CIBERSORT and GSVA were further performed in the TCGA cohort, and the results indicated that resting CD4 memory

T and Th1 cell infiltration were negatively correlated with TRIM27 expression. $CD4^+$ T cells can contribute to tumor regression and help cytotoxic T lymphocytes (CTLs) to target and eliminate tumor cells [36-38]. Our findings indicated the crucial role of TRIM27 in negatively regulating tumor-infiltrating immunocytes, which was rarely reported in the literature. Interestingly, an earlier study observed that TRIM27, through ubiquitinating the Class-II PI3K-C2β, inhibited cytokine production in primary human $CD4^+$ T cells [39]. These findings reconfirm our results that TRIM27 in immune cells can suppress immunity which is also consistent with our immunohistochemistry result that higher expression of TRIM27 in immune cells predicts a poorer prognosis.

To verify the distribution and functional mechanisms of TRIM27 in RCC, we further analyzed results at the single-cell level and found TRIM27 expressed in both tumor and immune cells, which was the same as immunohistochemistry-based findings. Since patients with highly expressed TRIM27 tumor cells presented lower $CD4^+$ T cell infiltration, its underlying molecular mechanisms on tumor cells were revealed; GSEA showed that "MTORC1 signaling", "MYC targets", and "glycolysis" pathways were highly enriched in highly expressed TRIM27 tumor cells. Previous studies found that TRIM27 could activate PI3K/AKT signaling and promote the EMT or carcinogenesis in colon and esophageal cancer cells, but the action of mTORC1 signaling had not been involved. In myocardial studies, TRIM27 was also found to promote cardiac hypertrophy via PTEN/Akt/mTOR [34]. mTOR signaling, as a pathway frequently activated in many cancers including colorectal cancers, can promote (glucose transporter 1) GLUT1 expression via the transcription factors myelocytomatosis (MYC) to increase glucose uptake for sustaining tumor cell growth and proliferation [40, 41]. In summary, high expression of TRIM27 on RCC cells may activate the mTORC1-MYC-glycolysis signaling pathway.

Many studies have shown that glucose uptake is required for proper immune response in both initial and activated T cell populations and a glucose-poor tumor microenvironment can mediate T cell hypo-responsiveness because of metabolic restrictions [42, 43]. Furthermore, inhibition of mTORC1 promotes differentiation of dendritic cells and enhances T cells via the Bruton's tyrosine kinase-indoleamine 2,3-dioxygenase axis, which also reflects a role that mTOR plays in anti-tumor immunity [44]. Together with our analysis, it was found that TRIM27 might increase tumor aerobic glycolysis via the mTOR pathway and result in a lower glucose tumor microenvironment and limitation of tumor-infiltrating T cell responses. Additionally, a glucose-deficient environment has differential effects on T cell subsets. Comparatively $CD8^+$ T cells have higher glycolytic flux and exhibit metabolic flexibility by oxidizing glutamine rapidly in a glucose-deficient environment. While $CD4^+$ T cells depend primarily on glucose as their oxidative fuel [45]. Thus, we inferred that $CD4^+$ T cells were more sensitive to changes in environmental glucose levels induced by TRIM27. It also explained why $CD4^+$ T cells were negatively regulated to the greatest extent in the highly expressed TRIM27 group.

We suppose that TRIM27 in RCC cells provides sufficient glucose energy for rapid cell proliferation through the mTORC1-MYC-glycolysis pathway based on GSEA analysis. However, the oncogenic activation of mTOR is also involved in the growth, survival, and proliferation of cancer cells through other mechanisms [46], which further complements the possible roles of TRIM27 in RCC. PI3K-mTORC1 signaling is required to promote lipogenesis by the activation of the pro-lipogenic factor SREBP1 and increasing lipid synthesis is a hallmark of proliferating cancer cells [47]. The increase of ribosome biogenesis is also associated with mTOR activation [48, 49]. Therefore, TRIM27-mTORC1 possibly promotes cell proliferation by providing various forms of energy to sustain high levels of cell growth. In addition, the activation of the mTORC1/4E-BP1/eIF4E signaling axis promotes the up-regulation of survivin expression [50], which may also be an important pathway activated by TRIM27 in RCC cells. Recently, Yang *et al*. found TRIM27 inhibited autophagy by polyubiquitinating ULK1 and promoted breast tumorigenesis in PyMT mice [51]. Autophagy is a double-edged sword in tumorigenesis and the activation of PI3K-mTORC1 signaling strongly inhibits autophagy in cancer cells [46]. Whether the autophagy mediated by mTORC1 is also regulated by TRIM27 is unclear now but autophagy deficiency induced by TRIM27 may be an important mechanism to accumulate damaged cellular parts and proteins and promote RCC tumorigenesis.

In addition, some reports stated that TRIM27 expressed in immune cells also affected the level of infiltration of T cells and $CD4^+$ T cells. Zaman *et al*. found that compared to wild-type, the TRIM27-/- mice induced by streptozotocin showed enhanced cleaved caspase-3 signals and increased infiltration of $CD3^+$ T cells in the pancreas [52]. They thought it was because TRIM27 positively regulated TNF-α-induced apoptosis through deubiquitination of receptor-interacting protein 1; in TRIM27-/- mice TNF-α-induced apoptosis was abrogated. Another independent study found TRIM27 decreased PI3K (phosphoinositide 3-kinase) activity through Lys48 polyubiquitination of PI3KC2β. It negatively regulated different $CD4^+$ T cells, including Jurkat, and activated human $CD4^+$ T cells, by inhibiting KCa3.1 channel activity and T cell receptor-stimulated Ca^{2+} influx [39]. These studies revealed two distinct mechanisms, which complemented our finding to the effect that TRIM27 in immune cells also inhibited $CD4^+$ T cell infiltration.

Genomic alterations and molecular subtypes are potential factors regulating tumor immunity [53]. BRAF mutation patients account for 8-12% of metastatic CRCs [54], which are characterized by poor prognosis and less benefit from anti-epidermal growth factor receptor antibody therapy [55, 56]. Chromosomal instability (CIN), as a central driver of tumor evolution, is associated with metastasis and therapeutic resistance and has proven to be a predictive marker for poorer survival outcome [57, 58]. RCC patients with the BRAF mutation or CIN subtype were more common in the highly expressed TRIM27 group, indicating that highly expressed TRIM27 patients were typified by stronger tumor aggressiveness and therapeutic resistance. TRIM27 was not only related to BRAF mutations but also correlated with the expression of immune checkpoint genes (PD1 and CTLA-4). This suggested that highly expressed TRIM27 patients might benefit from BRAF inhibitors (Vemurafenib) or immunotherapy [59].

In this study, we regarded RCC as an independent tumor and found that TRIM27 was an important biomarker for diagnosis, prognosis, and later-line therapy. However, TRIM27 failed to fully reflect the complexity of the TIME and needed to be used with other markers to predict the efficacy of immunotherapy in the future. Besides, we only used bioinformatics analyses to expound the carcinogenic and immune-suppressing mechanisms of TRIM27 but there was a lack of further experimental verification of our findings. Whether TRIM27 also predicted poorer prognosis and had the same function in the transverse colon, left-sided colon, and rectum was not explored.

In summary, TRIM27 is a promising immune-related prognostic biomarker for predicting the prognosis of RCC patients. It may exert its oncogenic effect by activating the mTORC1/glycolysis pathway and suppressing $CD4^+$ T cell infiltration, therefore it may be a viable therapeutic target. These results should be validated by more basic experiments and large clinical trials in the future.

Acknowledgements

The authors would like to acknowledge the Key Laboratory of Precision Diagnosis and Treatment of Gastrointestinal Tumors (China Medical University), Ministry of Education for providing the space and equipment for conducting the experiments. This work was supported by the National Natural Science Foundation of China (No.81972331); National Natural Science Foundation of China (No.31770963); High-level innovation and entrepreneurship team of Liaoning Province's "Xing Liao Talents Program" (XLYC2008006); "China Medical University-Chinese Academy of Sciences Shenyang Branch Scientist Partner" project (HZHB2022002); National Key Research and Development Plan of China (2020YFC2006401); High-level Talent Introduction Support Project (Project No.36003).

Disclosure of conflict of interest

None.

Address correspondence to: Ti Wen and Xiujuan Qu, Department of Medical Oncology, The First Hospital of China Medical University, Shenyang 110001, Liaoning, China. Tel: +86-15204027727; E-mail: wenti@cmu.edu.cn (TW); Tel: +86-13604031355; E-mail: xjqu@cmu.edu.cn (XJQ)

References

[1] Sung H, Ferlay J, Siegel RL, Laversanne M, Soerjomataram I, Jemal A and Bray F. Global cancer statistics 2020: GLOBOCAN estimates

of incidence and mortality worldwide for 36 cancers in 185 countries. CA Cancer J Clin 2021; 71: 209-249.
[2] Stintzing S, Tejpar S, Gibbs P, Thiebach L and Lenz HJ. Understanding the role of primary tumour localisation in colorectal cancer treatment and outcomes. Eur J Cancer 2017; 84: 69-80.
[3] Shen H, Yang J, Huang Q, Jiang MJ, Tan YN, Fu JF, Zhu LZ, Fang XF and Yuan Y. Different treatment strategies and molecular features between right-sided and left-sided colon cancers. World J Gastroenterol 2015; 21: 6470-6478.
[4] Modest DP, Schulz C, von Weikersthal LF, Quietzsch D, von Einem JC, Schalhorn A, Vehling-Kaiser U, Laubender RP, Giessen C, Stintzing S and Heinemann V. Outcome of patients with metastatic colorectal cancer depends on the primary tumor site (midgut vs. hindgut): analysis of the FIRE1-trial (FuFIRI or mIROX as first-line treatment). Anticancer Drugs 2014; 25: 212-218.
[5] Meguid RA, Slidell MB, Wolfgang CL, Chang DC and Ahuja N. Is there a difference in survival between right-versus left-sided colon cancers? Ann Surg Oncol 2008; 15: 2388-2394.
[6] Cremolini C, Antoniotti C, Moretto R, Masi G and Falcone A. First-line therapy for mCRC - the influence of primary tumour location on the therapeutic algorithm. Nat Rev Clin Oncol 2017; 14: 113.
[7] Di J, Zhuang M, Yang H, Jiang B, Wang Z and Su X. Clinical significance of circulating immune cells in left- and right-sided colon cancer. PeerJ 2017; 5: e4153.
[8] Huang Y, Ji L, Zhu J, Mao X, Sheng S, Hao S, Xiang D, Guo J, Fu G, Huang M, Lei Z and Chu X. Lymph node status and its impact on the prognosis of left-sided and right-sided colon cancer: a SEER population-based study. Cancer Med 2021; 10: 8708-8719.
[9] Mizuno R, Kawada K and Sakai Y. Prostaglandin E2/EP signaling in the tumor microenvironment of colorectal cancer. Int J Mol Sci 2019; 20: 6254.
[10] Mlecnik B, Tosolini M, Kirilovsky A, Berger A, Bindea G, Meatchi T, Bruneval P, Trajanoski Z, Fridman WH, Pages F and Galon J. Histopathologic-based prognostic factors of colorectal cancers are associated with the state of the local immune reaction. J Clin Oncol 2011; 29: 610-618.
[11] Pancione M, Giordano G, Remo A, Febbraro A, Sabatino L, Manfrin E, Ceccarelli M and Colantuoni V. Immune escape mechanisms in colorectal cancer pathogenesis and liver metastasis. J Immunol Res 2014; 2014: 686879.
[12] Lee GH, Malietzis G, Askari A, Bernardo D, Al-Hassi HO and Clark SK. Is right-sided colon cancer different to left-sided colorectal cancer? - a systematic review. Eur J Surg Oncol 2015; 41: 300-308.
[13] Zhang X, Zhao H, Shi X, Jia X and Yang Y. Identification and validation of an immune-related gene signature predictive of overall survival in colon cancer. Aging (Albany NY) 2020; 12: 26095-26120.
[14] Ozato K, Shin DM, Chang TH and Morse HC 3rd. TRIM family proteins and their emerging roles in innate immunity. Nat Rev Immunol 2008; 8: 849-860.
[15] Hatakeyama S. TRIM proteins and cancer. Nat Rev Cancer 2011; 11: 792-804.
[16] Gao D, Zhou Z and Huang H. miR-30b-3p inhibits proliferation and invasion of hepatocellular carcinoma cells via suppressing PI3K/Akt pathway. Front Genet 2019; 10: 1274.
[17] Horio M, Kato T, Mii S, Enomoto A, Asai M, Asai N, Murakumo Y, Shibata K, Kikkawa F and Takahashi M. Expression of RET finger protein predicts chemoresistance in epithelial ovarian cancer. Cancer Med 2012; 1: 218-229.
[18] Liu S, Tian Y, Zheng Y, Cheng Y, Zhang D, Jiang J and Li S. TRIM27 acts as an oncogene and regulates cell proliferation and metastasis in non-small cell lung cancer through SIX3-beta-catenin signaling. Aging (Albany NY) 2020; 12: 25564-25580.
[19] Ma L, Yao N, Chen P and Zhuang Z. TRIM27 promotes the development of esophagus cancer via regulating PTEN/AKT signaling pathway. Cancer Cell Int 2019; 19: 283.
[20] Yao Y, Liu Z, Cao Y, Guo H, Jiang B, Deng J and Xiong J. Downregulation of TRIM27 suppresses gastric cancer cell proliferation via inhibition of the Hippo-BIRC5 pathway. Pathol Res Pract 2020; 216: 153048.
[21] Zhang HX, Xu ZS, Lin H, Li M, Xia T, Cui K, Wang SY, Li Y, Shu HB and Wang YY. TRIM27 mediates STAT3 activation at retromer-positive structures to promote colitis and colitis-associated carcinogenesis. Nat Commun 2018; 9: 3441.
[22] Zhang Y, Feng Y, Ji D, Wang Q, Qian W, Wang S, Zhang Z, Ji B, Zhang C, Sun Y and Fu Z. TRIM27 functions as an oncogene by activating epithelial-mesenchymal transition and p-AKT in colorectal cancer. Int J Oncol 2018; 53: 620-632.
[23] Motegi Y, Katayama K, Sakurai F, Kato T, Yamaguchi T, Matsui H, Takahashi M, Kawabata K and Mizuguchi H. An effective gene-knockdown using multiple shRNA-expressing adenovirus vectors. J Control Release 2011; 153: 149-153.
[24] Bhattacharya S, Dunn P, Thomas CG, Smith B, Schaefer H, Chen J, Hu Z, Zalocusky KA, Shan-

kar RD, Shen-Orr SS, Thomson E, Wiser J and Butte AJ. ImmPort, toward repurposing of open access immunological assay data for translational and clinical research. Sci Data 2018; 5: 180015.

[25] Liu Y, Sethi NS, Hinoue T, Schneider BG, Cherniack AD, Sanchez-Vega F, Seoane JA, Farshidfar F, Bowlby R, Islam M, Kim J, Chatila W, Akbani R, Kanchi RS, Rabkin CS, Willis JE, Wang KK, McCall SJ, Mishra L, Ojesina AI, Bullman S, Pedamallu CS, Lazar AJ, Sakai R; Cancer Genome Atlas Research Network, Thorsson V, Bass AJ and Laird PW. Comparative molecular analysis of gastrointestinal adenocarcinomas. Cancer Cell 2018; 33: 721-735, e728.

[26] Yoshihara K, Shahmoradgoli M, Martinez E, Vegesna R, Kim H, Torres-Garcia W, Trevino V, Shen H, Laird PW, Levine DA, Carter SL, Getz G, Stemke-Hale K, Mills GB and Verhaak RG. Inferring tumour purity and stromal and immune cell admixture from expression data. Nat Commun 2013; 4: 2612.

[27] Newman AM, Liu CL, Green MR, Gentles AJ, Feng W, Xu Y, Hoang CD, Diehn M and Alizadeh AA. Robust enumeration of cell subsets from tissue expression profiles. Nat Methods 2015; 12: 453-457.

[28] Hanzelmann S, Castelo R and Guinney J. GSVA: gene set variation analysis for microarray and RNA-seq data. BMC Bioinformatics 2013; 14: 7.

[29] Charoentong P, Finotello F, Angelova M, Mayer C, Efremova M, Rieder D, Hackl H and Trajanoski Z. Pan-cancer immunogenomic analyses reveal genotype-immunophenotype relationships and predictors of response to checkpoint blockade. Cell Rep 2017; 18: 248-262.

[30] Imperial R, Ahmed Z, Toor OM, Erdogan C, Khaliq A, Case P, Case J, Kennedy K, Cummings LS, Melton N, Raza S, Diri B, Mohammad R, El-Rayes B, Pluard T, Hussain A, Subramanian J and Masood A. Comparative proteogenomic analysis of right-sided colon cancer, left-sided colon cancer and rectal cancer reveals distinct mutational profiles. Mol Cancer 2018; 17: 177.

[31] Lee HO, Hong Y, Etlioglu HE, Cho YB, Pomella V, Van den Bosch B, Vanhecke J, Verbandt S, Hong H, Min JW, Kim N, Eum HH, Qian J, Boeckx B, Lambrechts D, Tsantoulis P, De Hertogh G, Chung W, Lee T, An M, Shin HT, Joung JG, Jung MH, Ko G, Wirapati P, Kim SH, Kim HC, Yun SH, Tan IBH, Ranjan B, Lee WY, Kim TY, Choi JK, Kim YJ, Prabhakar S, Tejpar S and Park WY. Lineage-dependent gene expression programs influence the immune landscape of colorectal cancer. Nat Genet 2020; 52: 594-603.

[32] Wu R, Guo W, Qiu X, Wang S, Sui C, Lian Q, Wu J, Shan Y, Yang Z, Yang S, Wu T, Wang K, Zhu Y, Wang S, Liu C, Zhang Y, Zheng B, Li Z, Zhang Y, Shen S, Zhao Y, Wang W, Bao J, Hu J, Wu X, Jiang X, Wang H, Gu J and Chen L. Comprehensive analysis of spatial architecture in primary liver cancer. Sci Adv 2021; 7: eabg3750.

[33] Zhang X, Lan Y, Xu J, Quan F, Zhao E, Deng C, Luo T, Xu L, Liao G, Yan M, Ping Y, Li F, Shi A, Bai J, Zhao T, Li X and Xiao Y. CellMarker: a manually curated resource of cell markers in human and mouse. Nucleic Acids Res 2019; 47: D721-D728.

[34] Chen Y, Liu Z, Hu Z, Feng X and Zuo L. Tripartite motif 27 promotes cardiac hypertrophy via PTEN/Akt/mTOR signal pathways. Bioengineered 2022; 13: 8323-8333.

[35] Xing L, Tang X, Wu K, Huang X, Yi Y and Huan J. TRIM27 functions as a novel oncogene in non-triple-negative breast cancer by blocking cellular senescence through p21 ubiquitination. Mol Ther Nucleic Acids 2020; 22: 910-923.

[36] Borst J, Ahrends T, Babala N, Melief CJM and Kastenmuller W. CD4(+) T cell help in cancer immunology and immunotherapy. Nat Rev Immunol 2018; 18: 635-647.

[37] Sillito F, Holler A and Stauss HJ. Engineering CD4+ T cells to enhance cancer immunity. Cells 2020; 9: 1721.

[38] Xie Y, Akpinarli A, Maris C, Hipkiss EL, Lane M, Kwon EK, Muranski P, Restifo NP and Antony PA. Naive tumor-specific CD4(+) T cells differentiated in vivo eradicate established melanoma. J Exp Med 2010; 207: 651-667.

[39] Cai X, Srivastava S, Sun Y, Li Z, Wu H, Zuvela-Jelaska L, Li J, Salamon RS, Backer JM and Skolnik EY. Tripartite motif containing protein 27 negatively regulates CD4 T cells by ubiquitinating and inhibiting the class II PI3K-C2beta. Proc Natl Acad Sci U S A 2011; 108: 20072-20077.

[40] Gao S, Chen M, Wei W, Zhang X, Zhang M, Yao Y, Lv Y, Ling T, Wang L and Zou X. Crosstalk of mTOR/PKM2 and STAT3/c-Myc signaling pathways regulate the energy metabolism and acidic microenvironment of gastric cancer. J Cell Biochem 2018; [Epub ahead of print].

[41] Kasprzak A. Insulin-like growth factor 1 (IGF-1) signaling in glucose metabolism in colorectal cancer. Int J Mol Sci 2021; 22: 6434.

[42] Chapman NM, Boothby MR and Chi H. Metabolic coordination of T cell quiescence and activation. Nat Rev Immunol 2020; 20: 55-70.

[43] Ho PC, Bihuniak JD, Macintyre AN, Staron M, Liu X, Amezquita R, Tsui YC, Cui G, Micevic G, Perales JC, Kleinstein SH, Abel ED, Insogna KL, Feske S, Locasale JW, Bosenberg MW, Rathmell JC and Kaech SM. Phosphoenolpyruvate is a metabolic checkpoint of anti-tumor T cell responses. Cell 2015; 162: 1217-1228.

[44] Sharma MD, Pacholczyk R, Shi H, Berrong ZJ, Zakharia Y, Greco A, Chang CS, Eathiraj S, Kennedy E, Cash T, Bollag RJ, Kolhe R, Sadek R, McGaha TL, Rodriguez P, Mandula J, Blazar BR, Johnson TS and Munn DH. Inhibition of the BTK-IDO-mTOR axis promotes differentiation of monocyte-lineage dendritic cells and enhances anti-tumor T cell immunity. Immunity 2021; 54: 2354-2371, e2358.

[45] Palmer CS, Hussain T, Duette G, Weller TJ, Ostrowski M, Sada-Ovalle I and Crowe SM. Regulators of glucose metabolism in CD4(+) and CD8(+) T cells. Int Rev Immunol 2016; 35: 477-488.

[46] Laplante M and Sabatini DM. mTOR signaling in growth control and disease. Cell 2012; 149: 274-293.

[47] Duvel K, Yecies JL, Menon S, Raman P, Lipovsky AI, Souza AL, Triantafellow E, Ma Q, Gorski R, Cleaver S, Vander Heiden MG, MacKeigan JP, Finan PM, Clish CB, Murphy LO and Manning BD. Activation of a metabolic gene regulatory network downstream of mTOR complex 1. Mol Cell 2010; 39: 171-183.

[48] Wyant GA, Abu-Remaileh M, Frenkel EM, Laqtom NN, Dharamdasani V, Lewis CA, Chan SH, Heinze I, Ori A and Sabatini DM. NUFIP1 is a ribosome receptor for starvation-induced ribophagy. Science 2018; 360: 751-758.

[49] Gentilella A, Kozma SC and Thomas G. A liaison between mTOR signaling, ribosome biogenesis and cancer. Biochim Biophys Acta 2015; 1849: 812-820.

[50] Wang J, Ye Q and She QB. New insights into 4E-BP1-regulated translation in cancer progression and metastasis. Cancer Cell Microenviron 2014; 1: e331.

[51] Yang Y, Zhu Y, Zhou S, Tang P, Xu R, Zhang Y, Wei D, Wen J, Thorne RF, Zhang XD, Guan JL, Liu L, Wu M and Chen S. TRIM27 cooperates with STK38L to inhibit ULK1-mediated autophagy and promote tumorigenesis. EMBO J 2022; 41: e109777.

[52] Zaman MM, Shinagawa T and Ishii S. Trim27-deficient mice are susceptible to streptozotocin-induced diabetes. FEBS Open Bio 2013; 4: 60-64.

[53] Rooney MS, Shukla SA, Wu CJ, Getz G and Hacohen N. Molecular and genetic properties of tumors associated with local immune cytolytic activity. Cell 2015; 160: 48-61.

[54] Thorsson V, Gibbs DL, Brown SD, Wolf D, Bortone DS, Ou Yang TH, Porta-Pardo E, Gao GF, Plaisier CL, Eddy JA, Ziv E, Culhane AC, Paull EO, Sivakumar IKA, Gentles AJ, Malhotra R, Farshidfar F, Colaprico A, Parker JS, Mose LE, Vo NS, Liu J, Liu Y, Rader J, Dhankani V, Reynolds SM, Bowlby R, Califano A, Cherniack AD, Anastassiou D, Bedognetti D, Mokrab Y, Newman AM, Rao A, Chen K, Krasnitz A, Hu H, Malta TM, Noushmehr H, Pedamallu CS, Bullman S, Ojesina AI, Lamb A, Zhou W, Shen H, Choueiri TK, Weinstein JN, Guinney J, Saltz J, Holt RA, Rabkin CS; Cancer Genome Atlas Research Network, Lazar AJ, Serody JS, Demicco EG, Disis ML, Vincent BG and Shmulevich I. The immune landscape of cancer. Immunity 2018; 48: 812-830, e814.

[55] van Brummelen EMJ, de Boer A, Beijnen JH and Schellens JHM. BRAF mutations as predictive biomarker for response to anti-EGFR monoclonal antibodies. Oncologist 2017; 22: 864-872.

[56] Nakayama I, Hirota T and Shinozaki E. BRAF mutation in colorectal cancers: from prognostic marker to targetable mutation. Cancers (Basel) 2020; 12: 3236.

[57] Bakhoum SF and Cantley LC. The multifaceted role of chromosomal instability in cancer and its microenvironment. Cell 2018; 174: 1347-1360.

[58] Watanabe T, Kobunai T, Yamamoto Y, Matsuda K, Ishihara S, Nozawa K, Yamada H, Hayama T, Inoue E, Tamura J, Iinuma H, Akiyoshi T and Muto T. Chromosomal instability (CIN) phenotype, CIN high or CIN low, predicts survival for colorectal cancer. J Clin Oncol 2012; 30: 2256-2264.

[59] Kopetz S, Guthrie KA, Morris VK, Lenz HJ, Magliocco AM, Maru D, Yan Y, Lanman R, Manyam G, Hong DS, Sorokin A, Atreya CE, Diaz LA, Allegra C, Raghav KP, Wang SE, Lieu CH, McDonough SL, Philip PA and Hochster HS. Randomized trial of irinotecan and cetuximab with or without vemurafenib in BRAF-mutant metastatic colorectal cancer (SWOG S1406). J Clin Oncol 2021; 39: 285-294.

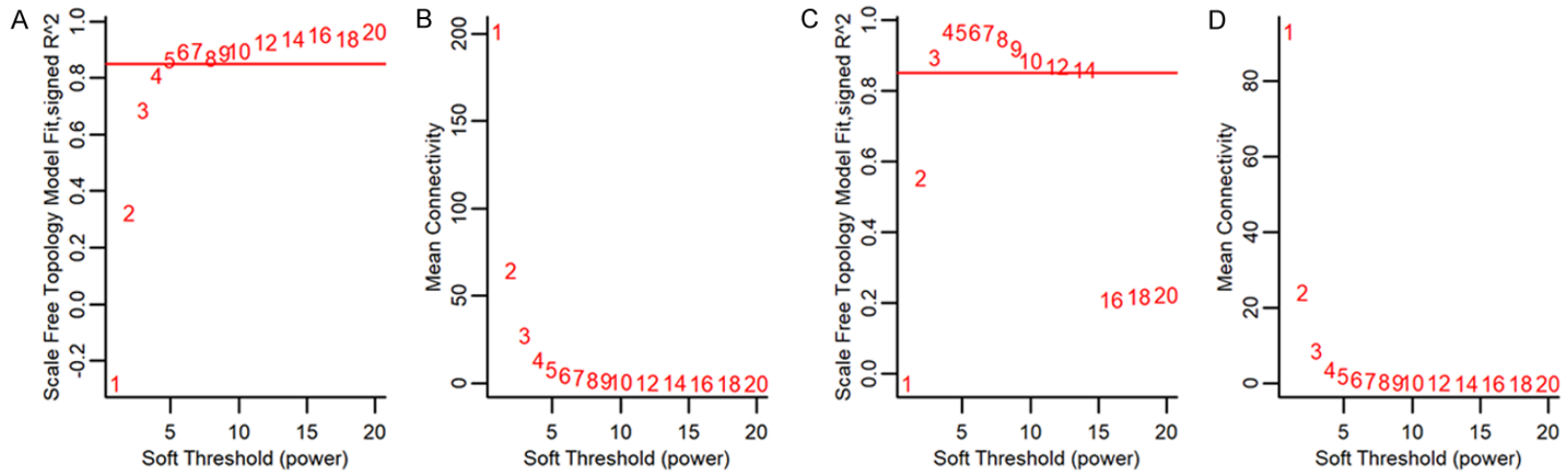

Figure S1. Determination of the soft-thresholding power in the WGCNA. A, B. In the TCGA cohort, the optimal soft threshold was five. C, D. In the GEO cohort, the optimal soft threshold was three.

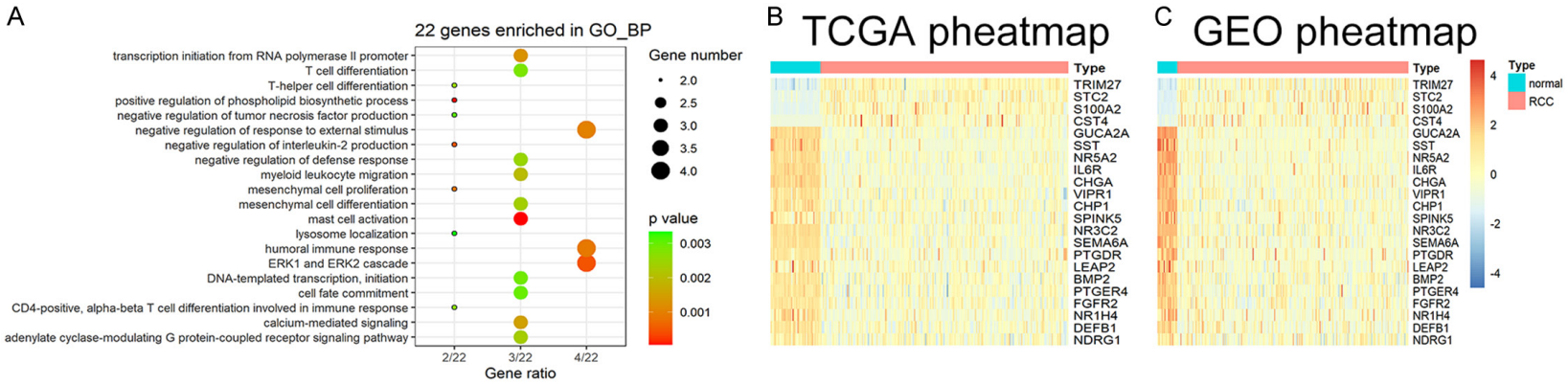

Figure S2. GO analysis and level of expression of 22 candidate genes. (A) GO pathways enriched in 22 candidate genes ($P < 0.05$). Heatmap of the expression level for 22 candidate genes in TCGA (B) and GEO (C) cohorts.

Table S1. The expression levels of 22 candidate genes in the TCGA and GSE39582 cohorts

Data sets	TCGA-RCC		GSE39582		Change
Gene	log2FC	FDR	FC	adj.P.Val	
TRIM27	1.152	3.72E-09	1.703	8.28E-14	Up
STC2	3.696	1.23E-42	2.477	1.58E-10	Up
S100A2	4.203	9.09E-37	5.054	2.56E-10	Up
CST4	6.812	8.03E-43	2.096	1.89E-05	Up
GUCA2A	-5.498	0	-58.389	4.67E-49	Down
SST	-5.078	1.35E-115	-10.531	2.69E-48	Down
NR5A2	-2.061	1.75E-28	-7.689	4.39E-42	Down
IL6R	-2.596	1.11E-50	-3.248	2.60E-38	Down
CHGA	-4.406	6.96E-197	-5.500	1.51E-29	Down
VIPR1	-1.515	1.29E-19	-4.525	1.51E-29	Down
CHP1	-1.075	6.44E-11	-6.574	9.71E-29	Down
SPINK5	-1.281	3.76E-08	-10.665	5.65E-26	Down
NR3C2	-2.330	7.76E-47	-11.327	5.65E-26	Down
SEMA6A	-2.155	2.47E-39	-6.503	1.66E-23	Down
PTGDR	-1.260	1.11E-07	-5.861	7.20E-22	Down
LEAP2	-1.138	1.75E-05	-2.709	1.32E-19	Down
BMP2	-1.550	1.89E-17	-5.239	1.04E-18	Down
PTGER4	-1.277	1.06E-12	-3.023	2.25E-16	Down
FGFR2	-1.788	5.14E-24	-1.894	5.99E-16	Down
NR1H4	-3.044	5.46E-44	-4.696	3.12E-12	Down
DEFB1	-2.279	4.08E-23	-4.074	1.72E-11	Down
NDRG1	-1.018	3.64E-09	-1.504	1.02E-03	Down

FC: Fold change. FDR: False-discovery rate.

Table S2. Univariate Cox regression analysis of 22 candidate genes

Gene	HR	HR. 95L	HR. 95H	*P*. value
TRIM27	2.527	1.235	5.170	0.011
STC2	1.191	0.983	1.443	0.075
S100A2	0.978	0.790	1.210	0.835
CST4	1.137	0.886	1.461	0.313
GUCA2A	0.917	0.807	1.041	0.179
SST	0.945	0.706	1.264	0.701
NR5A2	0.742	0.535	1.030	0.074
IL6R	0.953	0.692	1.312	0.767
CHGA	1.065	0.906	1.252	0.444
VIPR1	0.969	0.713	1.318	0.841
CHP1	0.932	0.573	1.514	0.775
SPINK5	0.897	0.672	1.197	0.460
NR3C2	0.810	0.623	1.054	0.117
SEMA6A	0.903	0.708	1.152	0.413
PTGDR	1.141	0.942	1.383	0.178
LEAP2	1.159	0.670	2.004	0.598
BMP2	0.947	0.735	1.220	0.672
PTGER4	0.797	0.603	1.054	0.111
FGFR2	0.947	0.746	1.204	0.658
NR1H4	0.780	0.567	1.073	0.126
DEFB1	0.925	0.776	1.101	0.381
NDRG1	1.037	0.788	1.366	0.794

HR: Hazard Ratio.

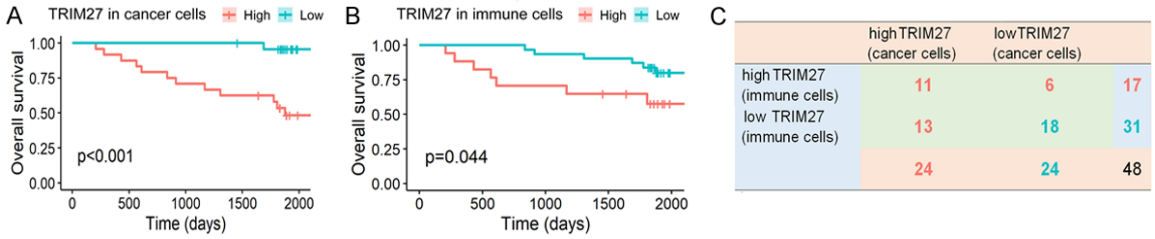

Figure S3. Survival analysis of TRIM27. Kaplan-Meier survival analyses separately based on the TRIM27 expression levels in cancer cells (A) and immune cells (B). (C) The number of patients with high and low levels of TRIM27.

Table S3. Correlation between TRIM27 and 28 kinds of lymphocytes

Cell type	Correlation coefficient	*P*. value
Activated B cell	-0.225	0.002
Mast cell	-0.224	0.002
Neutrophil	-0.178	0.015
Type1 T helper cell	-0.156	0.034
Eosinophil	-0.154	0.036
Memory B cell	-0.142	0.054
Type2 T helper cell	-0.142	0.055
Immature B cell	-0.141	0.055
Macrophage	-0.128	0.082
Natural killer cell	-0.127	0.086
Effector memory CD8 T cell	-0.122	0.098
Natural killer T cell	-0.112	0.128
Centra memory CD8 T cell	-0.107	0.147
Activated dendritic cell	-0.100	0.177
Type17 T helper cell	-0.095	0.199
CD56dim natural killer cell	0.088	0.234
Plasmacytoid dendritic cell	-0.080	0.278
Activated CD8 T cell	-0.074	0.314
Regulatory T cell	-0.066	0.372
T follicular helper cell	-0.059	0.422
Gamma delta T cell	-0.056	0.452
Effector memory CD4 T cell	-0.055	0.456
CD56bright natural killer cell	0.041	0.580
Myeloid derived suppressor cell	-0.032	0.666
Monocyte	-0.027	0.718
Central memory CD4 T cell	0.024	0.741
Activated CD4 T cell	0.013	0.859
Immature dendritic cell	-0.009	0.905

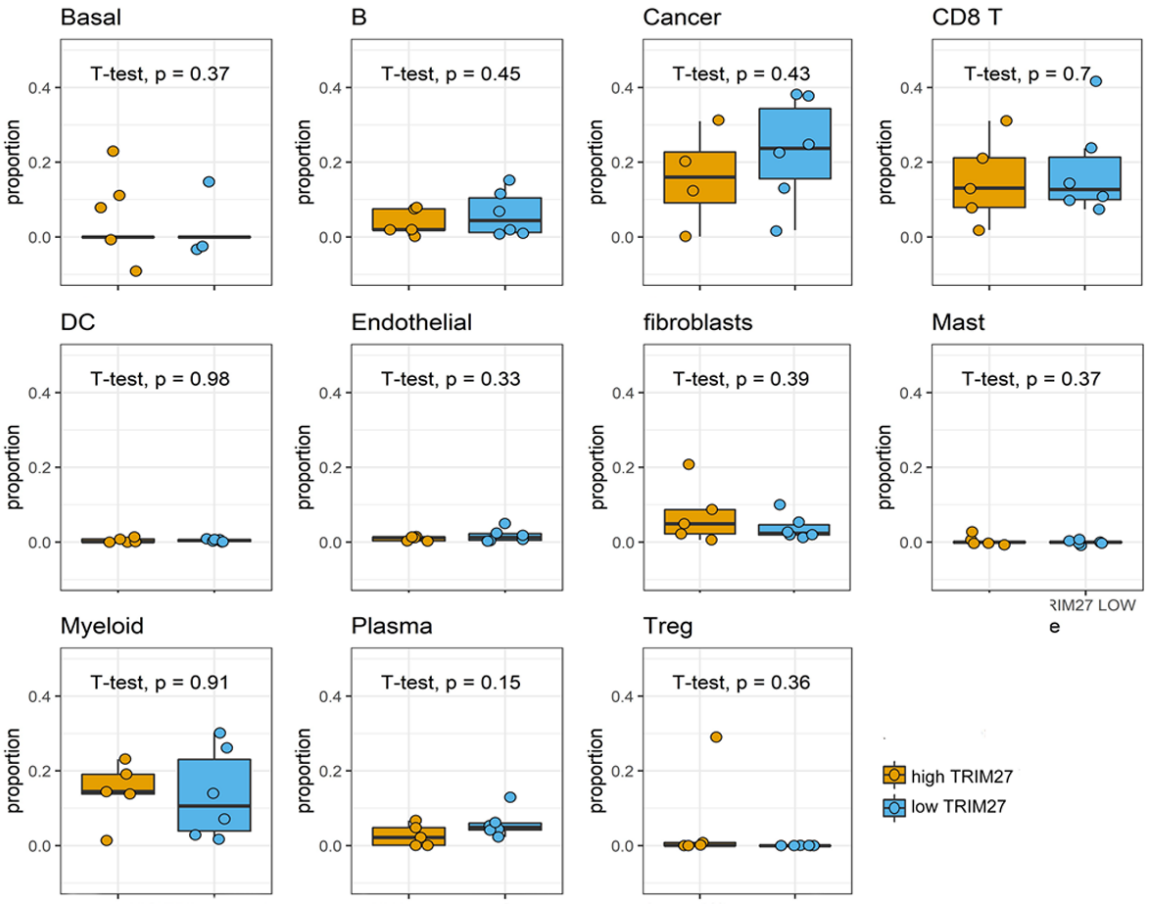

Figure S4. The proportions of various cell types in the patients with high and low levels of TRIM27 (differences were insignificant).

Table S4. Gene sets enriched in tumor cells with high TRIM27 expression

ID	NES	*P*. value	P. adjust	FDR
E2F_TARGETS	2.825	1.00E-10	1.00E-09	2.95E-10
MTORC1_SIGNALING	2.228	1.00E-10	1.00E-09	2.95E-10
MYC_TARGETS_V1	3.047	1.00E-10	1.00E-09	2.95E-10
OXIDATIVE_PHOSPHORYLATION	2.755	1.00E-10	1.00E-09	2.95E-10
TNFA_SIGNALING_VIA_NFKB	-2.897	1.00E-10	1.00E-09	2.95E-10
DNA_REPAIR	2.248	3.03E-09	2.52E-08	7.43E-09
ADIPOGENESIS	2.053	5.18E-08	3.70E-07	1.09E-07
G2M_CHECKPOINT	2.027	6.81E-08	4.26E-07	1.25E-07
EPITHELIAL_MESENCHYMAL_TRANSITION	-2.069	7.73E-08	4.29E-07	1.27E-07
FATTY_ACID_METABOLISM	2.040	5.80E-07	2.90E-06	8.54E-07
MYC_TARGETS_V2	2.151	5.61E-06	2.44E-05	7.19E-06
HYPOXIA	-1.903	5.86E-06	2.44E-05	7.19E-06
BILE_ACID_METABOLISM	2.034	1.30E-05	4.65E-05	1.37E-05
XENOBIOTIC_METABOLISM	1.859	1.30E-05	4.65E-05	1.37E-05
INFLAMMATORY_RESPONSE	-1.905	1.68E-05	5.61E-05	1.65E-05
IL6_JAK_STAT3_SIGNALING	-2.064	2.11E-05	6.61E-05	1.95E-05
ESTROGEN_RESPONSE_EARLY	-1.756	7.14E-05	2.10E-04	6.19E-05
P53_PATHWAY	-1.692	2.10E-04	5.82E-04	1.72E-04
APICAL_JUNCTION	-1.666	1.06E-03	2.80E-03	8.24E-04

PEROXISOME	1.743	1.20E-03	3.00E-03	8.85E-04
ESTROGEN_RESPONSE_LATE	-1.590	1.43E-03	3.41E-03	1.00E-03
MYOGENESIS	-1.628	2.09E-03	4.75E-03	1.40E-03
IL2_STAT5_SIGNALING	-1.596	2.21E-03	4.79E-03	1.41E-03
APOPTOSIS	-1.564	3.71E-03	7.73E-03	2.28E-03
UV_RESPONSE_DN	-1.600	4.98E-03	9.97E-03	2.94E-03
UNFOLDED_PROTEIN_RESPONSE	1.501	9.90E-03	0.019	5.61E-03
COMPLEMENT	-1.427	0.012	0.023	6.65E-03
KRAS_SIGNALING_UP	-1.463	0.014	0.025	7.40E-03
TGF_BETA_SIGNALING	-1.512	0.016	0.027	7.97E-03
APICAL_SURFACE	-1.586	0.017	0.028	8.18E-03
REACTIVE_OXYGEN_SPECIES_PATHWAY	1.603	0.018	0.028	8.18E-03
INTERFERON_ALPHA_RESPONSE	1.441	0.018	0.028	8.18E-03
GLYCOLYSIS	1.266	0.035	0.052	0.015
UV_RESPONSE_UP	-1.384	0.035	0.052	0.015
HEME_METABOLISM	-1.329	0.043	0.061	0.018
ANGIOGENESIS	-1.473	0.050	0.069	0.020
HEDGEHOG_SIGNALING	-1.408	0.089	0.121	0.036
NOTCH_SIGNALING	-1.391	0.095	0.126	0.037
KRAS_SIGNALING_DN	-1.269	0.107	0.137	0.040
COAGULATION	-1.193	0.131	0.163	0.048
SPERMATOGENESIS	1.229	0.152	0.185	0.055
ANDROGEN_RESPONSE	-1.147	0.221	0.263	0.077
PANCREAS_BETA_CELLS	1.178	0.230	0.268	0.079
CHOLESTEROL_HOMEOSTASIS	1.132	0.238	0.270	0.080
INTERFERON_GAMMA_RESPONSE	-1.058	0.329	0.366	0.108
MITOTIC_SPINDLE	-1.024	0.381	0.414	0.122
WNT_BETA_CATENIN_SIGNALING	1.022	0.407	0.433	0.128
ALLOGRAFT_REJECTION	-1.014	0.429	0.447	0.132
PI3K_AKT_MTOR_SIGNALING	0.935	0.595	0.607	0.179
PROTEIN_SECRETION	0.784	0.885	0.885	0.261

NES: Normalized enrichment score. FDR: False-discovery rate.

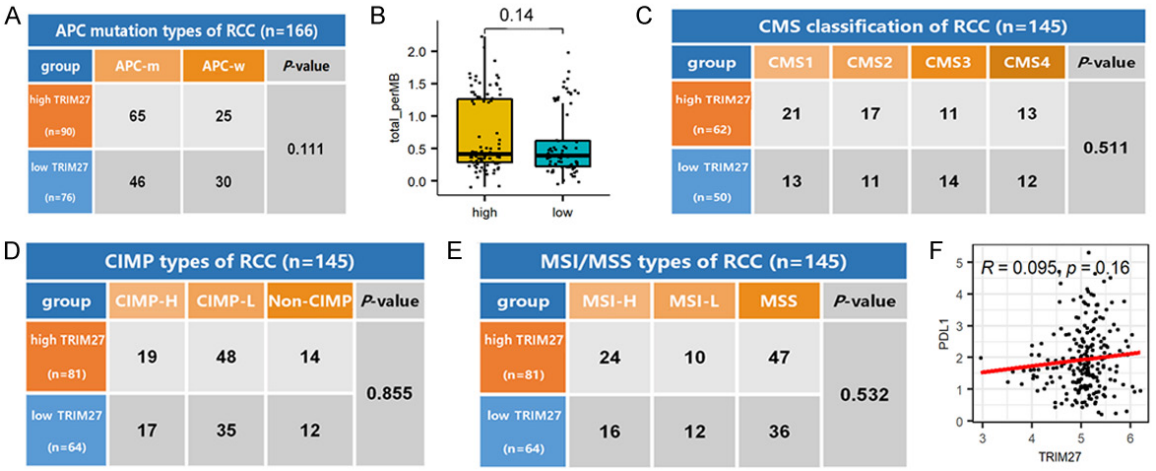

Figure S5. Molecular characteristics of the groups of high and low levels of TRIM27. The distribution of APC mutation subtypes (A), TMB (B), CMS classification (C), CIMP classification (D), and MSI/MSS classification (E) in the highly and lowly expressed groups of TRIM27. Correlation between TRIM27 and expression level of PDL1 (F).